Life Sciences 232 (2019) 116501

Contents lists available at ScienceDirect

Life Sciences

journal homepage: www.elsevier.com/locate/lifescie

Multiple functional therapeutic effects of DL-3-n-butylphthalide in the cuprizone model of demyelination

Yuejuan Wu, Le Dong, Qi Huang, Lanfeng Sun, Yuhan Liao, Yulan Tang*, Yuan Wu*

Department of Neurology, The First Affiliated Hospital of Guangxi Medical University, Nanning, Guangxi, China

ARTICLE INFO

Keywords:
Multiple sclerosis
DL-3-n-butylphthalide
Corpus callosum
Neuroinflammation
Nuclear factor-κB

ABSTRACT

Aims: Multiple sclerosis (MS) is a chronic inflammatory demyelinating disease of the central nervous system (CNS). The disease mechanisms driving progressive MS remain unresolved. Without this information, current therapeutic strategies are unsatisfactory in preventing disease progression. Our previous work revealed that DL-3-n-butylphthalide (NBP) treatment reduced demyelination in an ethidium bromide mouse model of demyelination. Here, we examine the effect of NBP in the cuprizone model of demyelination by evaluating the pathologic, functional, and behavioral consequences of treatment with NBP.

Materials and methods: Forty mice were divided randomly into 4 groups: a normal diet group, a cuprizone diet group, and two NBP groups (10 and 20 mg/kg). CNS infiltration by microglia, axon health and myelination were assessed using immunohistochemistry and electron microscopy, and the levels of cytoplasmic complexes were assessed by Western blotting.

Key findings: The results showed the neuroprotective effects of the NBP included suppressing the microglia activation through inhibition of nuclear factor-κB (NF-κB) expression, thus decreasing activation of the NF-κB signaling pathway. In particular, myelin density was increased due to an increased mean number of mature oligodendrocytes (OLs) in the high-dose NBP (20 mg/kg) subgroup through reduced oligodendrocyte apoptosis. Meanwhile, increased expression of myelin sheath proteins, including proteolipid protein (PLP) and myelin basic protein (MBP), was observed in the same subgroup.

Significance: These data suggest that NBP may not only have anti-inflammatory properties but also promote the survival of OLs in a mouse cuprizone model of demyelination. NBP may have a potential role in the treatment of MS.

1. Introduction

Multiple sclerosis (MS) is a chronic inflammatory demyelinating disease of the central nervous system (CNS) that results from immune-mediated inflammation, demyelination and subsequent axonal damage [1–3]. The incidence of MS [4] varies among different locations (range, 15/100000 to 250/100000). Clinically, 60–80% of patients experience relapse and progress to chronic conditions with motor disability and cognitive deficits. Previous studies have suggested that MS lesions are dominated by inflammation, but this inflammation occurs partly on the brain side of the blood-brain barrier, which makes it more difficult to treat.

Cuprizone, a copper-chelating agent, can induce demyelination in multiple parts of the CNS, especially the corpus callosum [5]. This toxic model of demyelination has two main features: increased oligodendrocyte (OL) degeneration via mitochondrial injury [6,7] and secretion of pro-inflammatory cytokines [8]. In particular, the blood-brain barrier remains intact during cuprizone treatment.

DL-3-n-butylphthalide (NBP) a family of optical isomers comprising L-3-N-butylphthalide (L-NBP) and D-3-N-butylphthalide (D-NBP), is extracted from Chinese celery and is ordinarily used to treat acute ischemic stroke in China [9]. Previous studies have shown that NBP suppresses inflammatory responses, oxidative damage, and neuronal apoptosis in an animal model of middle cerebral artery occlusion [10–12]. Research has also shown that NBP prolongs survival in an animal model of amyotrophic lateral sclerosis (ALS) by reducing glial cell activation and decreasing motor neuron death [13,14].

Recently, we reported that NBP improved symptoms, electroencephalogram (EEG) features, and brain magnetic resonance imaging (MRI) in a patient with demyelination and showed an antiapoptotic

* Corresponding authors at: Department of Neurology, The First Affiliated Hospital of Guangxi Medical University, Nanning 530021, Guangxi Zhuang Autonomous Region, China.

E-mail addresses: tangyulan7@163.com (Y. Tang), wuyuan90@126.com (Y. Wu).

https://doi.org/10.1016/j.lfs.2019.05.057
Received 21 February 2019; Received in revised form 8 May 2019; Accepted 21 May 2019
Available online 01 June 2019

effect in the ethidium bromide model of demyelination [15]; however, the mechanisms are still not well understood. Therefore, we explore the mechanisms by which NBP reduces demyelination in the cuprizone toxic model of demyelination.

2. Materials and methods

2.1. Cuprizone model of demyelination

Male C57BL/6 mice with body weights ranging between 17 and 20 g (6 weeks old) were obtained from the Animal Experiment Center of Medical University. Their housing room was maintained on a 12 h light:12 h dark cycle at a temperature between 20 and 22 °C. The mice also had free access to water and food. For the purpose of inducing demyelination, mice were fed ground, powdered standard rodent chow containing 0.2% cuprizone for 5 weeks. Control animals were fed normal powdered chow. All experiments were conducted according to the National Institutes of Health (NIH) Guide for the Care and Use of Laboratory Animals.

2.2. Experimental design

Mice were divided randomly into 3 groups: (i) a control group that received normal powdered chow for 5 weeks with intraperitoneal (i.p.) injection of 0.9% saline for the last 4 weeks of that period; (ii) a cuprizone group that received powdered chow mixed with 0.2% cuprizone for 5 weeks; and (iii) an NBP (CSPC NBP Pharmaceutical Co. Ltd., China) plus cuprizone group, which was divided into 2 separate subgroups, treated with 10 or 20 mg/kg of NBP by i.p. injection for the last 4 weeks of the 5-week feeding period. All mice from the three groups were evaluated through behavioral, molecular, and histopathological tests.

2.3. Behavioral experiments

2.3.1. Rotarod test

A rotarod test was conducted using a rotor with a 5.7-cm diameter (47650 Rota-Rod NG, Ugo Basile, USA). In brief, mice received two training sessions spaced two days apart during the 5th week of cuprizone feeding. After the training session, mice were placed on the rod, which rotated at 40 rpm for 10 min. The latency to fall was automatically recorded by magnetic trip plates. Each mouse was tested three times, and the mean latency was calculated.

2.3.2. Western blot analysis

The caudal region of the corpus callosum was isolated from the brain, then homogenized and centrifuged at 12000 rpm for 15 min with lysis buffer containing a complete protease inhibitor mixture. Protein concentrations were measured with a bicinchoninic acid assay and standardized. The total protein was separated by 12% SDS PAGE and transferred to polyvinylidene fluoride membranes. The membranes were blocked for 1 h with 5% fat-free milk in TBST buffer and then incubated with the primary antibodies including anti-Bax (#2772, CST), anti-Cleaved Caspase-3 (#9661, CST), anti-TNF-α (#11948, CST), anti-NF-κB p65 (#8242, CST), anti-Bcl-2 (ab59348, Abcam), anti-IκBα (ab32518, Abcam), anti-tubulin-β (#33532, SAB), anti-Lamin B1(#41589-1, SAB), anti-PLP (#C00944, SAB), anti-MBP (#21640-2, SAB), anti-GAPDH (10494-1, Proteintech Group) at 4 °C overnight. The membranes were washed and subsequently exposed to the appropriate horseradish peroxidase-conjugated secondary antibodies (#L3012-2, SAB) for 1 h at room temperature. After three washes in TBST, immunoreactive peptides were detected by ECL kit (Shanghai Tian Neng Technology Co. Ltd). The results were quantified by densitometric scanning of films, and Image J was used to measure the integrated density of the bands after subtracting the background. Nuclear and cytoplasmic proteins were isolated as described.

2.4. Histopathological studies

2.4.1. Electron microscopy and analysis of demyelination

After the rotarod test，mice were perfused with 0.9% saline for 3 or 5 min, followed by 10% glutaraldehyde plus 4% paraformaldehyde. Following perfusion, the corpus callosum was removed and postfixed in 4% glutaraldehyde for 2 h. After three rinses in 0.1 mol/L phosphate-buffered saline (PBS), the specimens were dehydrated in an ascending ethanol series (70%, 80%, 90%, 96%, and 100%) followed by acetone (100%, water-free). Then, the blocks were trimmed, processed, and embedded in resin. Ultrathin sections (60 nm) were cut using an ultramicrotome (Leica EM UC7, Leica Microsystems, Wetzlar, Germany). These sections were used for light microscopy and for electron microscopy (EM) on a Hitachi H-7650 transmission electron microscope. Images were captured with a VELETA digital camera using Olympus Soft Imaging Solutions.

2.4.2. Paraffin Section Method and Technique

Mice treated with 5% chloral hydrate (i.p., 0.1 mL/10 g) were perfused with 0.9% saline for 3–5 min, followed by 4% paraformaldehyde (PFA). Coronal sections from brains fixed in 4% PFA and embedded in paraffin for 24 h were obtained in 3- and 6-μm thicknesses.

2.4.3. TUNEL test and immunofluorescent staining

Terminal deoxynucleotidyl transferase-mediated dUTP nick-end labeling (TUNEL) and immunofluorescent staining were used to evaluate oligodendrocyte cell apoptosis in paraffinized sections. After dehydration, the sections were subjected to high-pressure antigen retrieval with citric acid buffer (pH 6.0), rinsed with PBS solution, and blocked with 10% goat serum and 1% Triton X-100 in PBS. Subsequently, the sections were incubated with anti-APC antibody (1:100, ab15270, Abcam) at 4 °C overnight. The tissues were then incubated in TUNEL (Cat. No. 11684817910, Roche) reaction mixture (450 μL of label solution and 50 μL of enzyme solution) and anti-rabbit IgG (H + L), F(ab')2 fragment (Alexa Fluor 594 conjugate, #8889, CST), at 37 °C for 60 min. The specimens were mounted using Solarbio mounting medium with 4′,6-diamidino-2-phenylindole (DAPI). The numbers of TUNEL-positive (green) and APC-positive (red) neurons were calculated in each specimen (two visual fields/specimen). The sections were analyzed by immunofluorescence microscopy (BX53; Olympus, Japan).

2.4.4. Luxol Fast Blue (LFB) staining

LFB staining was applied to paraffin sections to assess myelination. After dehydration, brain sections were incubated with LFB solution (G3240, Beijing Solarbio Science & Technology Co.) at room temperature overnight. The slides were differentiated in Luxol differentiation solution for 15 s and then in 70% ethyl alcohol for another 30 s after being rinsed with 95% ethanol, 70% ethanol and distilled water. Following another wash with distilled water, the sections were counterstained with eosin for 1 min. Thereafter, the sections were washed with distilled water, dehydrated in a graded alcohol series, cleared in xylene, and finally mounted. The ventral body of the corpus callosum was observed with an Olympus light microscope (BX53, Olympus, Japan) and photographed with an Olympus digital camera linked to the microscope. ImageJ software was used to evaluate the extent of demyelination based on the volume ratio of blue to pink fibers in the corpus callosum of each animal, representing the proportion of damaged tissue.

2.4.5. Hematoxylin and Eosin (H&E) staining

Furthermore, inflammation was assessed by H&E staining. H&E staining was used to assess the severity of inflammation at the lesion site. The sections were stained with hematoxylin for 5 min. After being washed with water, the sections were counterstained with eosin for 1 min, rehydrated with a graded alcohol series, and cleared with xylene. The specimens were viewed with an Olympus BX53 microscope (Japan)

and photographed with an Olympus digital camera linked to the microscope. ImageJ software was used to evaluate the extent of inflammatory cell infiltration as the proportion of inflammatory cells in a given field.

2.4.6. Immunohistochemical procedures for Ibal-1

Furthermore, inflammation was assessed by immunohistochemical procedures for Ibal-1 to stained microglia. After dehydration, the sections were subjected to high-pressure antigen retrieval with citric acid buffer (pH 6.0), rinsed with PBS solution, and blocked with 10% goat serum and 1% Triton X-100 in PBS. Subsequently, the sections were incubated with anti-Ibal-1 antibody (1:1000, ab178847, Abcam) at 4 °C overnight. Negative controls were conducted by exchange of primary antibody for PBS. Sections were then incubated with the horseradish peroxidase-conjugated secondary antibody (#L3012-2, SAB), and finally incubated with diaminobenzidin (DAB) at room temperature for 3–5 min. The specimens were viewed with an Olympus BX53 microscope (Japan) and photographed with an Olympus digital camera linked to the microscope. Image J software was used to calculate the numbers of microglia as the proportion of inflammatory cells in the corpus callosum.

2.5. Statistical analysis

For all experiments, we used SPSS 21.0 to analyze data. The statistical significance of the differences was assessed using one-way ANOVA, followed by pairwise *t*-tests with a Bonferroni correction. A value of $P < 0.05$ was considered statistically significant.

3. Results

3.1. The effect of NBP on motor skills

After being trained for the task, mice were tested for their latency to fall from the rotarod. The latency was (37.38 ± 38.34) for the cuprizone group ($n = 8$) and (214.13 ± 90.52) for the control group (n = 8, $P < 0.05$). The latency reduction associated with cuprizone was attenuated in both of the NBP plus cuprizone subgroups (n = 8 per group; $P < 0.05$, Fig. 1). There was no statistical difference between the two NBP groups ($P > 0.05$).

3.2. The effect of NBP on NF-κB, IκBα, and TNF-α levels

H&E staining and Ibal-1 immunohistochemistry staining were performed to test the level of tissue inflammation, using inflammatory cells and microglia as indicators. The number of infiltrating inflammatory cells and microglia were increased in the cuprizone group compared with those in the control group (Fig. 2A–D). We also investigated the effect of NBP in the two NBP plus cuprizone subgroups. NBP (10 mg/kg and 20 mg/kg) treatment, compared with cuprizone treatment alone, dose-dependently decreased the abundance of infiltrating inflammatory cells and microglia. There were significant differences between the two NBP groups in the infiltrating inflammatory cells ($P < 0.01$) and microglia ($P < 0.01$). Next, we assessed the effect of NBP on the potential NF-κB pathway in three groups by Western blotting. Increased NF-κB expression was observed in the cuprizone group (Fig. 3A and B). In contrast, the levels of NF-κB in the two NBP plus cuprizone subgroups were reduced significantly in a dose-dependent manner. Next, we assessed the level of the cytoplasmic inhibitory protein IκBα, an upstream signaling protein that can regulate the activity of NF-κB, as well as the expression of tumor necrosis factor alpha (TNF-α), a downstream component that is one of the inflammatory response markers produced by activated NF-κB. The data suggested that there was considerably more degradation of IκBα in the cuprizone group than in the control group. Moreover, there was a dose-dependent improvement in IκBα levels in the two NBP plus cuprizone subgroups compared with the cuprizone group (Fig. 3C). This result was consistent with the NF-κB levels. Significant decreases in TNF-α were observed in the two NBP plus cuprizone subgroups compared with the cuprizone group (Fig. 3D).

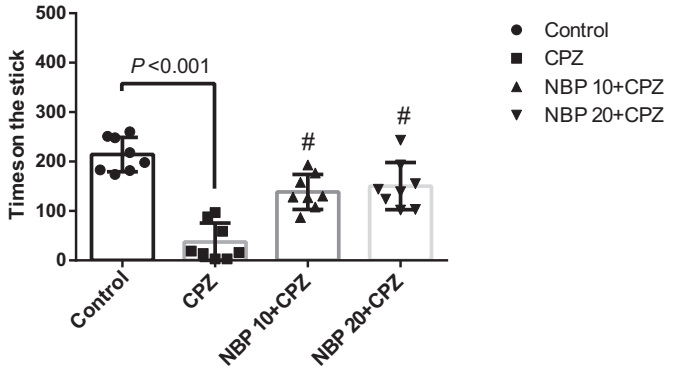

Fig. 1. Rotarod performance and NBP treatment. Mice treated with NBP at 10 mg/kg or 20 mg/kg remained on the rotarod longer than the cuprizone group. Data represent the mean ± SD. #$P < 0.05$ versus cuprizone group.

3.3. The effect of NBP on mature OL survival

Significantly increased OL apoptosis was observed in the cuprizone group compared with the control group and the high-dose NBP subgroup (Fig. 4A). The ration of Bax to Bcl-2 and the level of active caspase-3 are two key markers in the regulation of apoptosis. In the cuprizone group, the caspase-3 level and the Bax/Bcl-2 ratio were increased, while NBP treatment decreased caspase-3 expression and the Bax/Bcl-2 ratio in the high-dose NBP subgroup (Fig. 4B and C).

3.4. The effect of NBP on myelination

LFB staining and EM were used to assess the integrity of axonal myelin sheaths. Through LFB staining, significant demyelination was observed in the cuprizone group compared with the control group. Furthermore, obviously increased myelin density and numbers of myelinated axons were observed in the NBP plus cuprizone group, as shown in Fig. 5A and C. In EM, the numbers of nonmyelinated axons and thinly myelinated callosal fibers were increased in the cuprizone group (Fig. 5B). The number of nonmyelinated axons was decreased in the NBP plus cuprizone group. Meanwhile, there were significant differences in demyelination between the NBP group and the cuprizone group (Fig. 5C). And then, we also investigated the levels of demyelination between the two NBP subgroups. The data showed that there was a statistical difference between the two NBP groups ($P < 0.001$). The levels of PLP and MBP, two indicators of the myelination process, were examined in the three groups (Fig. 6). The expression levels of these proteins were significantly reduced by cuprizone treatment compared with the expression in the control group. In contrast, the levels of PLP and MBP expression were significantly improved in the 20 mg/kg NBP plus cuprizone subgroup.

4. Discussion

Management of MS is one of the challenges that must be confronted in the new century. To date, three therapeutic strategies have been proposed: anti-inflammatory therapy, remyelination therapy, and neuroprotective therapy [16–18].

NBP, a chiral compound from Chinese celery seed extract, has shown neuroprotective effects and anti-inflammatory effects in Alzheimer's disease [19,20], Parkinson's disease [21], ALS [22], stroke [23,24], and dementia [25,26]. Recently, we reported that NBP ameliorated demyelination in a case of heroin abuse and further

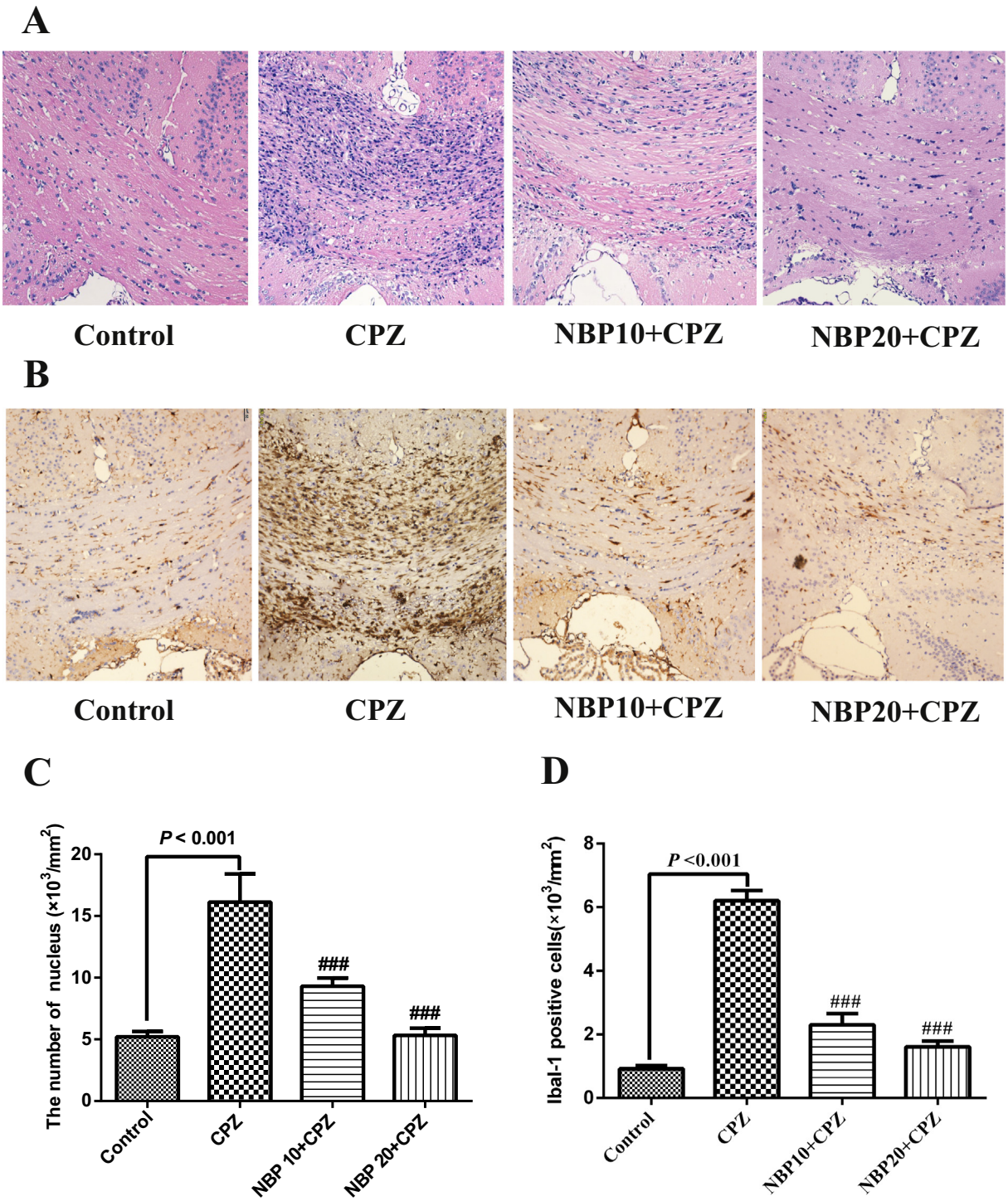

Fig. 2. H&E staining and Ibal-1 immunohistochemistry staining results are presented. Feeding cuprizone significantly increased the level of inflammatory cell and microglia infiltration in the corpus callosum. Treatment with NBP at 10 mg/kg or 20 mg/kg, compared to cuprizone treatment alone, significantly reduced the abundance of inflammatory cell and microglia in a dose-dependent manner. Data represent the mean ± SD. The scale bar equals 50 μm. *###P* < 0.001 versus the cuprizone group.

demonstrated that NBP reduced demyelinating lesions in callosal white matter in an ethidium bromide mouse model of demyelination [27], which indicated that NBP might be a promising agent for MS treatment.

The present study provided evidence that NBP improved the latency in the rotarod test in the cuprizone group, indicating that NBP can ameliorate cuprizone-induced behavioral dysfunctions. The protective effect of NBP was similar to that reported in an experimental mouse model of ALS [22]. However, there was no difference in the latency between the two NBP subgroups. We infer that the heterogeneity of mice, such as biological features of the host, may help partly explain similar results between the two NBP subgroups.

NF-κB, which is a family of transcription factors regulated by IκBα degradation, is considered a primary regulator of inflammatory processes. Previous studies have shown that IκBα degradation can cause NF-κB to translocate to the nucleus, resulting in the expression of a large variety of pro-inflammatory genes, such as TNF-α and IL-1. The

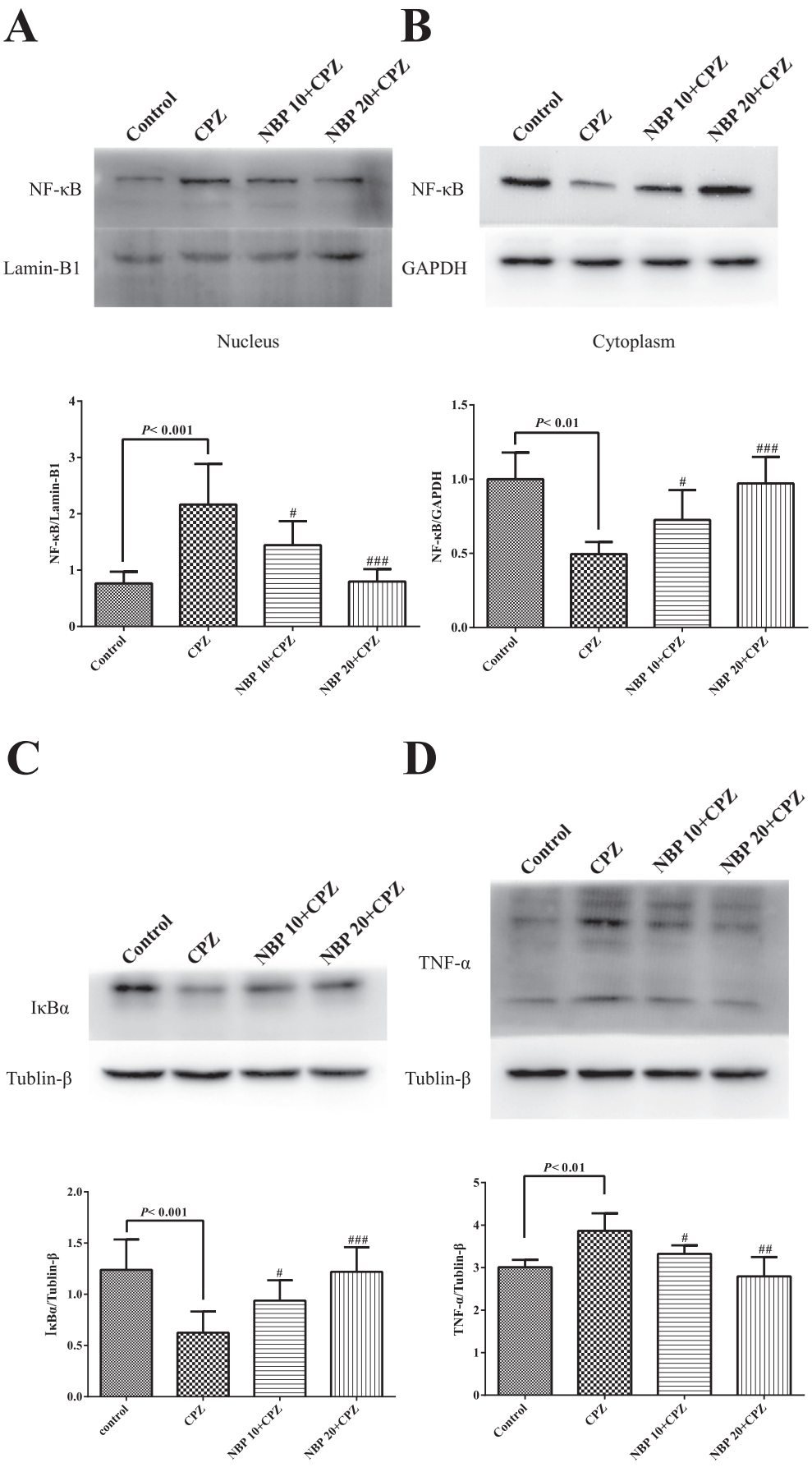

Fig. 3. Effect of NBP application on NF-κB and IκBα levels in cuprizone-treated mice. Western blot analysis shows NF-κB and IκBα levels in the corpus callosum in the different groups. NF-κB and IκBα bands were measured to calculate the ratios to Lamin B1 or GAPDH for NF-κB and tubulin-β for IκBα. (A) In the nucleus, NF-κB levels were decreased dose-dependently in the two NBP plus cuprizone subgroups compared with the cuprizone group. (B) In the cytoplasm, there were significant differences between the two NBP plus cuprizone subgroups and the cuprizone group. (C) A significant increase in IκBα levels occurred in the two NBP plus cuprizone subgroups compared with the cuprizone group. (D) NBP treatment decreases TNF-α levels in NBP plus cuprizone mice in a dose-dependent manner. $\#P < 0.05$ versus the cuprizone group, $\#\#P < 0.01$ versus the cuprizone group, $\#\#\#P < 0.001$ versus the cuprizone group.

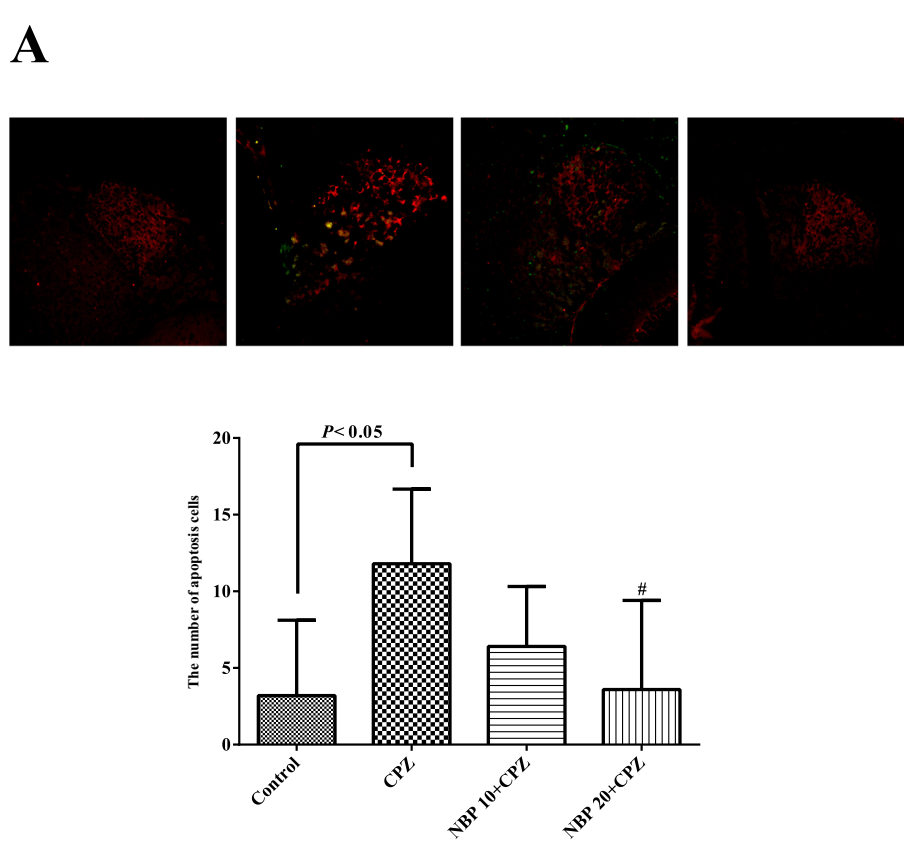

Fig. 4. A high dose of NBP increases the survival of OLs in cuprizone-treated mice. Increased OL apoptosis (green mixed with red) in the cuprizone group was observed. An increase in APC (red) immunostaining revealed improved mature OL numbers in the high-dose NBP-treated groups (A). Western blot analysis revealed that high-dose NBP treatment diminished the Bax/Bcl-2 ratio and decreased caspase-3 expression compared with those of the cuprizone group (B and C). $\#P < 0.05$ versus the cuprizone group, $\#\#P < 0.01$ versus the cuprizone group. (For interpretation of the references to colour in this figure legend, the reader is referred to the web version of this article.)

proteins translated from these gene transcripts can damage and kill OLs in the cuprizone model of demyelination [28]. Furthermore, researchers have reported that the anti-inflammatory effect of NBP is partially based on inhibition of the NF-κB signaling pathway [29]. In our results, NBP suppressed cuprizone-induced IκBα degradation and NF-κB nuclear translocation to a remarkable extent, leading to a

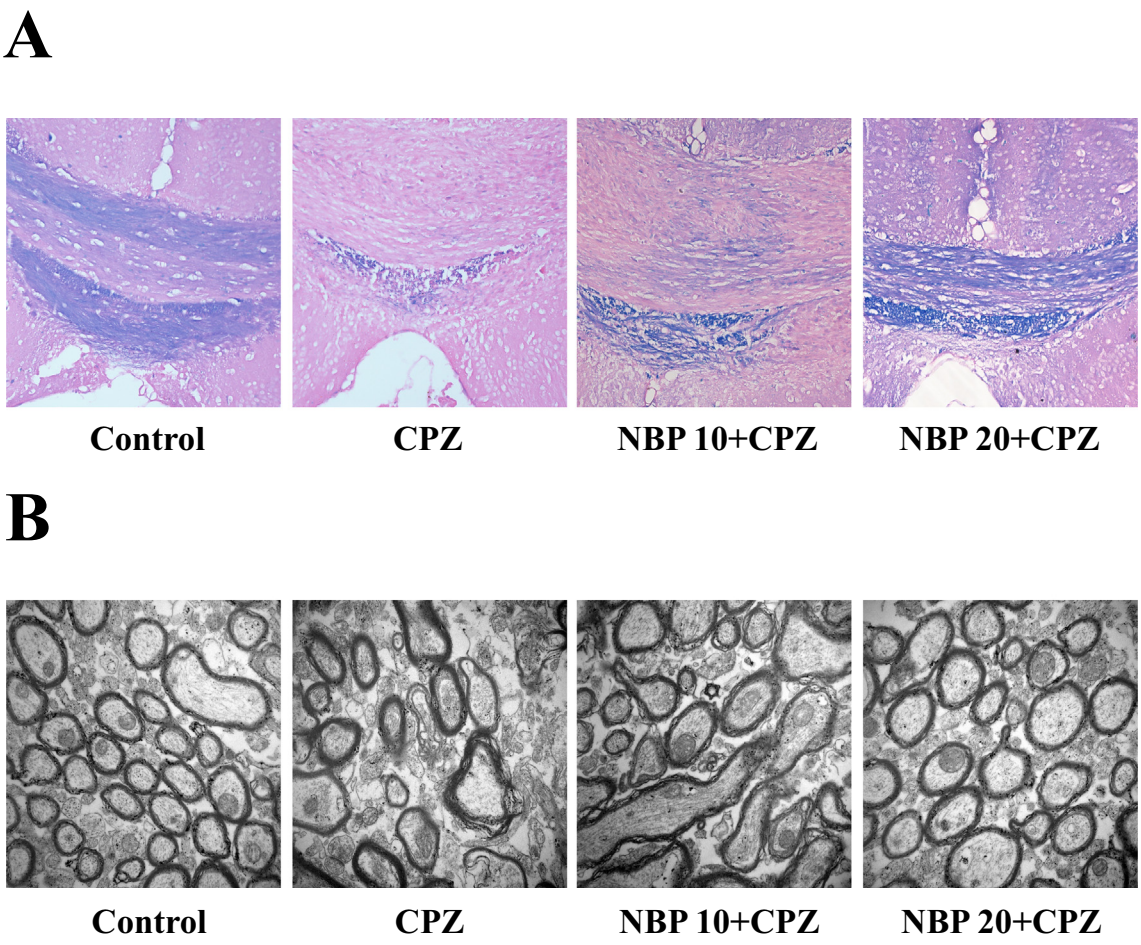

Fig. 5. Assessment of myelin integrity in the corpus callosum with LFB staining (A and C). Intact regions are stained blue, while demyelinate areas are stained pink. There was significant demyelination in the cuprizone group compared with the control group. Demyelination was reduced by NBP treatment. These results were consistent with those of EM (B). $###P < 0.001$ versus the cuprizone group. (For interpretation of the references to colour in this figure legend, the reader is referred to the web version of this article.)

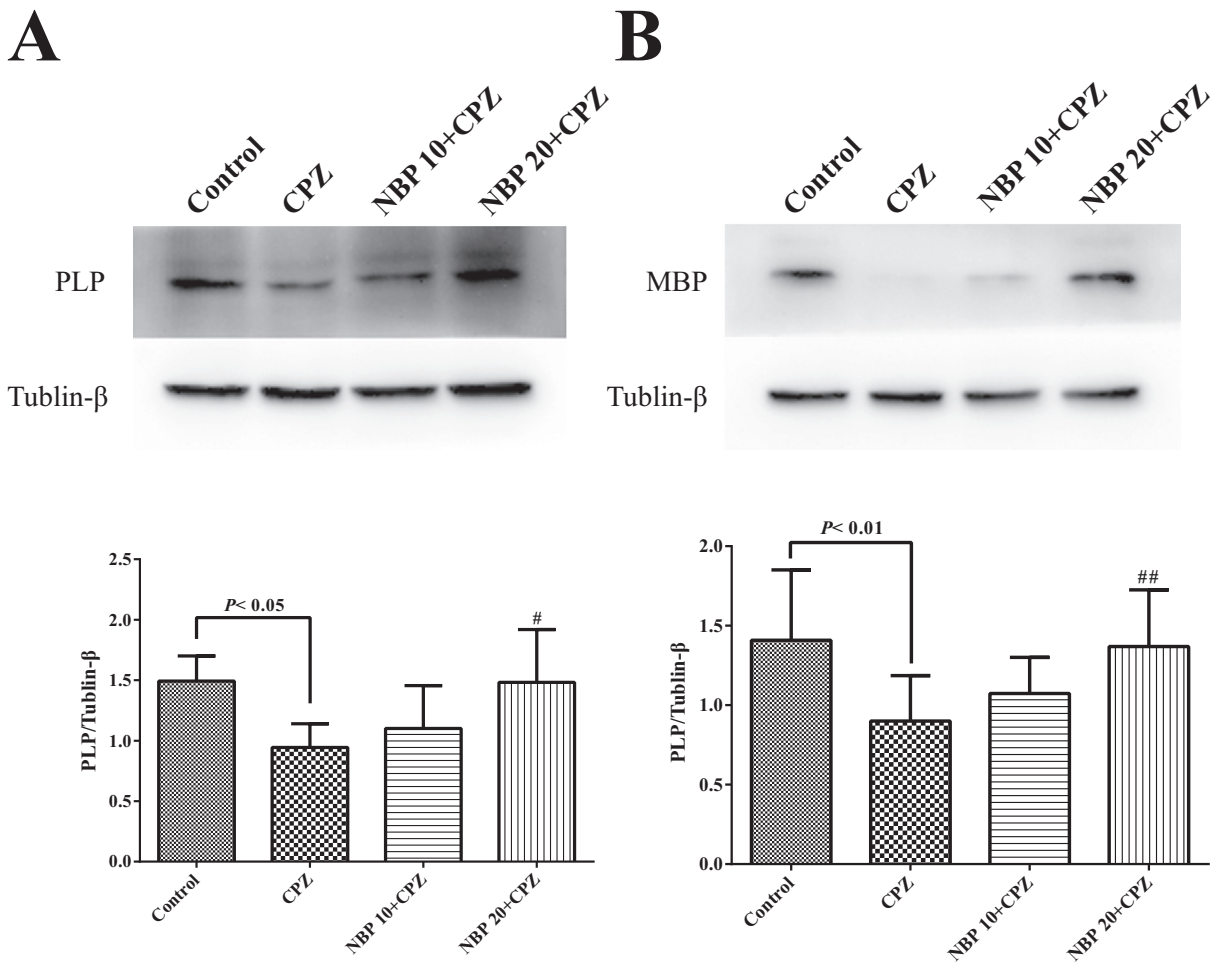

Fig. 6. Effect of NBP application on myelin protein (PLP and MBP) levels in cuprizone-treated mice. The levels of PLP and MBP expression in the different groups were assessed through Western blot analysis by calculating the ratios of the PLP (A) and MBP (B) bands to the tubulin-β band. There was no statistically significant difference in PLP or MBP expression between the low-dose NBP subgroup and the cuprizone group. In contrast, a significant increase was observed in the high-dose NBP subgroup. $\#P < 0.05$ versus the cuprizone group, $\#\#P < 0.01$ versus the cuprizone group.

substantial decrease in the inflammatory response. This result coincided with reductions in both cuprizone-induced peripheral immune response and microglia increases, demonstrating immunomodulatory capabilities of NBP. Meanwhile, high-dose NBP also showed better immunomodulatory capabilities than low-dose NBP in the present study.

The death of glial cells, especially oligodendrocytes, plays a critical role in the pathophysiology of MS [30]. Dying oligodendrocytes release stored Fe^{2+} into the parenchyma, where the ions can amplify oxidative damage by producing oxidants, suggesting that OL apoptosis contributes to demyelination and axonal damage in the cuprizone model [31]. Our study demonstrated that NBP decreased OL apoptosis in mice with cuprizone-induced demyelination. Bax and Bcl-2, of the B cell lymphoma 2 protein family, have long been known to have an important role in the regulation of mitochondrial membrane permeability and apoptosis [32], and caspase-3 is well known as a downstream executioner caspase that functions in caspase-dependent apoptotic cascades [33]. Therefore, we examined these proteins as major players in the regulation of apoptosis. Specifically, NBP inhibited caspase-3 activity, leading to increased numbers of OLs. Furthermore, NBP diminished the Bax/Bcl-2 ratio via an increase in Bcl-2 and a decrease in Bax, which is further evidence of NBP's ability to regulate cuprizone-induced apoptosis through the mitochondrial-dependent intrinsic pathway. This aspect of NBP will be further clarified in future studies.

In addition, the expression levels of mRNAs for myelin proteins, including MBP, PLP, MAG, and CGT, increased during the first two weeks and returned to normal levels between weeks 3 and 6 under continuous cuprizone exposure [34]. These mRNAs and their corresponding proteins remained detectable after 6 weeks of continuous cuprizone exposure [35]. In this study, we found that the protein expression of PLP and MBP was significantly decreased in the cuprizone group. The difference between our data and those reported in other studies might be due to different regenerative properties of different brain regions. We used specimens from the corpus callosum. In contrast, tissues from half of a midsagittally sectioned brain were used in other studies. Furthermore, we showed that the levels of PLP and MBP expression were upregulated in the high-dose NBP group, while the low dose of NBP did not affect this process although demyelination were decreased in the low-dose NBP subgroup. This result suggests that a high dose of NBP is capable of reducing demyelination in the cuprizone model, possibly by promoting the formation of myelin protein, and might be worth prioritizing for effective MS therapy.

Conclusions

In conclusion, this study indicates that NBP may be a promising agent for MS, and its neuroprotective effects may be ascribed to suppression of inflammation through inhibition of the NF-κB signaling pathway and promoting the survival of OLs.

Author contributions

YLT and YW contributed to the conception and design of the work. YJW, LD and LFS performed most of the experiments. QH and YHL performed the data analysis. YJW and YW contributed to the drafting of the report. All authors contributed to the revision of the manuscript, and all authors read and approved the submitted version.

Declaration of Competing Interest

The Authors declare that there are no conflicts of interest.

Acknowledgments

This study was supported by a grant from Guangxi Natural Science Foundation Program (03201215060D).

Appendix A. Supplementary data

Supplementary data to this article can be found online at https://doi.org/10.1016/j.lfs.2019.05.057.

References

[1] A. Compston, A. Coles, Multiple sclerosis, Lancet 372 (2008) 1502–1517, https://doi.org/10.1016/S0140-6736(08)61620-7.
[2] E.M. Frohman, M.K. Racke, C.S. Raine, Multiple sclerosis—the plaque and its pathogenesis, N. Engl. J. Med. 354 (2006) 942–955, https://doi.org/10.1056/NEJMra052130.
[3] L. Steinman, Multiple sclerosis: a two-stage disease, Nat. Immunol. 2 (2001) 762–764, https://doi.org/10.1038/ni0901-762.
[4] E. Kingwell, J.J. Marriott, N. Jette, T. Pringsheim, N. Makhani, S.A. Morrow, J.D. Fisk, C. Evans, S.G. Beland, S. Kulaga, J. Dykeman, C. Wolfson, M.W. Koch, R.A. Marrie, Incidence and prevalence of multiple sclerosis in Europe: a systematic review, BMC Neurol. 13 (2013) 128, https://doi.org/10.1186/1471-2377-13-128.
[5] T. Skripuletz, J.H. Bussmann, V. Gudi, P.N. Koutsoudaki, R. Pul, D. Moharregh-Khiabani, M. Lindner, M. Stangel, Cerebellar cortical demyelination in the murine cuprizone model, Brain Pathol. 20 (2010) 301–312, https://doi.org/10.1111/j.1750-3639.2009.00271.x.
[6] L. Messori, A. Casini, C. Gabbiani, L. Sorace, M. Muniz-Miranda, P. Zatta, Unravelling the chemical nature of copper cuprizone, Dalton Trans. (2007) 2112–2114, https://doi.org/10.1039/b701896g.
[7] W. Cammer, The neurotoxicant, cuprizone, retards the differentiation of oligodendrocytes in vitro, J. Neurol. Sci. 168 (1999) 116–120.
[8] L.A. Pasquini, C.A. Calatayud, A.L. Bertone Una, V. Millet, J.M. Pasquini, E.F. Soto, The neurotoxic effect of cuprizone on oligodendrocytes depends on the presence of pro-inflammatory cytokines secreted by microglia, Neurochem. Res. 32 (2007) 279–292, https://doi.org/10.1007/s11064-006-9165-0.
[9] H. Zhao, W. Yun, Q. Zhang, X. Cai, X. Li, G. Hui, X. Zhou, J. Ni, Mobilization of circulating endothelial progenitor cells by dl-3-n-butylphthalide in acute ischemic stroke patients, J. Stroke Cerebrovasc. Dis. 25 (2016) 752–760, https://doi.org/10.1016/j.jstrokecerebrovasdis.2015.11.018.
[10] G.X. Dong, Y.P. Feng, [Effects of NBP on ATPase and anti-oxidant enzymes activities and lipid peroxidation in transient focal cerebral ischemic rats]. Zhongguo yi xue ke xue yuan xue bao, Acta Acad. Med. Sinicae 24 (2002) 93–97.
[11] Q. Chang, X.L. Wang, Effects of chiral 3-n-butylphthalide on apoptosis induced by transient focal cerebral ischemia in rats, Acta Pharmacol. Sin. 24 (2003) 796–804.
[12] H.L. Xu, Y.P. Feng, Inhibitory effects of chiral 3-n-butylphthalide on inflammation following focal ischemic brain injury in rats, Acta Pharmacol. Sin. 21 (2000) 433–438.
[13] Q.M. Zhou, J.J. Zhang, S. Li, S. Chen, W.D. Le, N-butylidenephthalide treatment prolongs life span and attenuates motor neuron loss in SOD1(G93A) mouse model of amyotrophic lateral sclerosis, CNS Neurosci. Ther. 23 (2017) 375–385, https://doi.org/10.1111/cns.12681.
[14] X.H. Feng, W. Yuan, Y. Peng, M.S. Liu, L.Y. Cui, Therapeutic effects of dl-3-n-butylphthalide in a transgenic mouse model of amyotrophic lateral sclerosis, Chin. Med. J. 125 (2012) 1760–1766.
[15] Y. Wu, Q. Huang, X. Liu, X. Wei, Dl-3-n-butylphthalide is effective for demyelination: a case-combined study, Clin. Neurol. Neurosurg. 137 (2015) 83–88, https://doi.org/10.1016/j.clineuro.2015.06.024.
[16] X. Montalban, S.L. Hauser, L. Kappos, D.L. Arnold, A. Bar-Or, G. Comi, J. de Seze, G. Giovannoni, H.P. Hartung, B. Hemmer, F. Lublin, K.W. Rammohan, K. Selmaj, A. Traboulsee, A. Sauter, D. Masterman, P. Fontoura, S. Belachew, H. Garren, N. Mairon, P. Chin, J.S. Wolinsky, Ocrelizumab versus placebo in primary progressive multiple sclerosis, N. Engl. J. Med. 376 (2017) 209–220, https://doi.org/10.1056/NEJMoa1606468.
[17] A.J. Green, J.M. Gelfand, B.A. Cree, C. Bevan, W.J. Boscardin, F. Mei, J. Inman, S. Arnow, M. Devereux, A. Abounasr, H. Nobuta, A. Zhu, M. Friessen, R. Gerona, H.C. von Budingen, R.G. Henry, S.L. Hauser, J.R. Chan, Clemastine fumarate as a remyelinating therapy for multiple sclerosis (ReBUILD): a randomised, controlled, double-blind, crossover trial, Lancet 390 (2017) 2481–2489, https://doi.org/10.1016/S0140-6736(17)32346-2.
[18] R. Raftopoulos, S.J. Hickman, A. Toosy, B. Sharrack, S. Mallik, D. Paling, D.R. Altmann, M.C. Yiannakas, P. Malladi, R. Sheridan, P.G. Sarrigiannis, N. Hoggard, M. Koltzenburg, C.A. Gandini Wheeler-Kingshott, K. Schmierer, G. Giovannoni, D.H. Miller, R. Kapoor, Phenytoin for neuroprotection in patients with acute optic neuritis: a randomised, placebo-controlled, phase 2 trial, Lancet Neurol. 15 (2016) 259–269, https://doi.org/10.1016/S1474-4422(16)00004-1.
[19] C.Y. Wang, Z.Y. Wang, J.W. Xie, T. Wang, X. Wang, Y. Xu, J.H. Cai, Dl-3-n-butylphthalide-induced upregulation of antioxidant defense is involved in the enhancement of cross talk between CREB and Nrf2 in an Alzheimer's disease mouse model, Neurobiol. Aging 38 (2016) 32–46, https://doi.org/10.1016/j.neurobiolaging.2015.10.024.
[20] C. Fernandez-Moriano, E. Gonzalez-Burgos, M.P. Gomez-Serranillos, Mitochondria-targeted protective compounds in Parkinson's and Alzheimer's diseases, Oxidative Med. Cell. Longev. 2015 (2015) 408927, https://doi.org/10.1155/2015/408927.
[21] N. Xiong, J. Huang, C. Chen, Y. Zhao, Z. Zhang, M. Jia, L. Hou, H. Yang, X. Cao, Z. Liang, Y. Zhang, S. Sun, Z. Lin, T. Wang, Dl-3-n-butylphthalide, a natural antioxidant, protects dopamine neurons in rotenone models for Parkinson's disease, Neurobiol. Aging 33 (2012) 1777–1791, https://doi.org/10.1016/j.neurobiolaging.2011.03.007.
[22] X. Feng, Y. Peng, M. Liu, L. Cui, DL-3-n-butylphthalide extends survival by attenuating glial activation in a mouse model of amyotrophic lateral sclerosis, Neuropharmacology 62 (2012) 1004–1010, https://doi.org/10.1016/j.neuropharm.2011.10.009.
[23] L. Zhang, W.H. Yu, Y.X. Wang, C. Wang, F. Zhao, W. Qi, W.M. Chan, Y. Huang, M.S. Wai, J. Dong, D.T. Yew, DL-3-n-Butylphthalide, an anti-oxidant agent, prevents neurological deficits and cerebral injury following stroke per functional analysis, magnetic resonance imaging and histological assessment, Curr. Neurovasc. Res. 9 (2012) 167–175.
[24] L.X. Xue, T. Zhang, Y.W. Zhao, Z. Geng, J.J. Chen, H. Chen, Efficacy and safety comparison of DL-3-n-butylphthalide and cerebrolysin: effects on neurological and behavioral outcomes in acute ischemic stroke, Exp. Ther. Med. 11 (2016) 2015–2020, https://doi.org/10.3892/etm.2016.3139.
[25] J. Jia, C. Wei, J. Liang, A. Zhou, X. Zuo, H. Song, L. Wu, X. Chen, S. Chen, J. Zhang, J. Wu, K. Wang, L. Chu, D. Peng, P. Lv, H. Guo, X. Niu, Y. Chen, W. Dong, X. Han, B. Fang, M. Peng, D. Li, Q. Jia, L. Huang, The effects of DL-3-n-butylphthalide in patients with vascular cognitive impairment without dementia caused by subcortical ischemic small vessel disease: a multicentre, randomized, double-blind, placebo-controlled trial, Alzheimers Dement. 12 (2016) 89–99, https://doi.org/10.1016/j.jalz.2015.04.010.
[26] Y. Huai, Y. Dong, J. Xu, N. Meng, C. Song, W. Li, P. Lv, L-3-n-butylphthalide protects against vascular dementia via activation of the Akt kinase pathway, Neural Regen. Res. 8 (2013) 1733–1742, https://doi.org/10.3969/j.issn.1673-5374.2013.19.001.
[27] A. Ozturk, S.A. Smith, E.M. Gordon-Lipkin, D.M. Harrison, N. Shiee, D.L. Pham, B.S. Caffo, P.A. Calabresi, D.S. Reich, MRI of the corpus callosum in multiple sclerosis: association with disability, Mult. Scler. 16 (2010) 166–177, https://doi.org/10.1177/1352458509353649.
[28] J. Raasch, N. Zeller, G. van Loo, D. Merkler, A. Mildner, D. Erny, K.P. Knobeloch, J.R. Bethea, A. Waisman, M. Knust, D. Del Turco, T. Deller, T. Blank, J. Priller, W. Bruck, M. Pasparakis, M. Prinz, IkappaB kinase 2 determines oligodendrocyte loss by non-cell-autonomous activation of NF-kappaB in the central nervous system, Brain 134 (2011) 1184–1198, https://doi.org/10.1093/brain/awq359.
[29] H.M. Wang, T. Zhang, J.K. Huang, X.J. Sun, 3-N-butylphthalide (NBP) attenuates the amyloid-beta-induced inflammatory responses in cultured astrocytes via the nuclear factor-kappaB signaling pathway, Cell. Physiol. Biochem. 32 (2013) 235–242, https://doi.org/10.1159/000350139.
[30] W. Bruck, R. Pfortner, T. Pham, J. Zhang, L. Hayardeny, V. Piryatinsky, U.K. Hanisch, T. Regen, D. van Rossum, L. Brakelmann, K. Hagemeier, T. Kuhlmann, C. Stadelmann, G.R. John, N. Kramann, C. Wegner, Reduced astrocytic NF-kappaB activation by laquinimod protects from cuprizone-induced demyelination, Acta Neuropathol. 124 (2012) 411–424, https://doi.org/10.1007/s00401-012-1009-1.
[31] H. Lassmann, J. van Horssen, D. Mahad, Progressive multiple sclerosis: pathology and pathogenesis, Nat. Rev. Neurol. 8 (2012) 647–656, https://doi.org/10.1038/nrneurol.2012.168.
[32] Y. Fuchs, H. Steller, Programmed cell death in animal development and disease, Cell 147 (2011) 742–758, https://doi.org/10.1016/j.cell.2011.10.033.
[33] J.F. Negron, R.A. Lockshin, Activation of apoptosis and caspase-3 in zebrafish early gastrulae, Dev. Dyn. 231 (2004) 161–170, https://doi.org/10.1002/dvdy.20124.
[34] P. Morell, C.V. Barrett, J.L. Mason, A.D. Toews, J.D. Hostettler, G.W. Knapp, G.K. Matsushima, Gene expression in brain during cuprizone-induced demyelination and remyelination, Mol. Cell. Neurosci. 12 (1998) 220–227, https://doi.org/10.1006/mcne.1998.0715.
[35] M. Lindner, S. Heine, K. Haastert, N. Garde, J. Fokuhl, F. Linsmeier, C. Grothe, W. Baumgartner, M. Stangel, Sequential myelin protein expression during remyelination reveals fast and efficient repair after central nervous system demyelination, Neuropathol. Appl. Neurobiol. 34 (2008) 105–114, https://doi.org/10.1111/j.1365-2990.2007.00879.x.